SYNTHESIS OF TRÖGER'S BASE LINKED DIBENZO-CROWN ETHER POLYMERS AND THEIR USE AS GAS SEPARATION MEMBRANES

by

CREIGHTON WILSON EDWARD BALTIER

JASON E. BARA, COMMITTEE CHAIR
STEVEN T. WEINMAN
PAUL A. RUPAR

A THESIS

Submitted in partial fulfillment of the requirements
for the degree of Master of Science
in the Department of Chemical and Biological Engineering
in the Graduate School of
The University of Alabama

TUSCALOOSA, ALABAMA

2022

ABSTRACT

Current methods of CO_2 separation are expensive to install and maintain for current industries and are inefficient in their carbon capture capabilities. In this work, a dibenzo-crown ether Tröger's Base (TB)-linked polymer was synthesized and tested as a gas separation membrane with measurements made for CO_2 and H_2 gas. The results show that the carbon dioxide permeability is affected by the ether groups due to the gas permeability being soluble controlled.

Further testing was performed to validate the credibility of the membrane's selectivity of carbon dioxide over other common gases in comparison to other similar membranes. Testing of single-strand dibenzene ether membranes along with membranes that replace the ether groups with alkane groups is advised for the collection of data warranted for the consideration of the future membranes.

Research for the foreseeable future will incorporate considerations of membrane physical properties, gas selectivity, synthesis consistency, and polymerization methods to lead to a greater understanding of membrane potential in carbon dioxide gas separation. The true capacity of membranes to solve the problem of carbon capture will only be revealed with further research developments.

DEDICATION

This thesis is dedicated to all who helped and encouraged me throughout my education at The University of Alabama, providing the opportunity to obtain the skills and mindset to complete my education. My family and friends especially helped me along this journey and I cannot thank them enough.

LIST OF ABBREVIATIONS AND SYMBOLS

Carbon Dioxide (CO_2)

Tröger's Base (TB)

Dibenzo-18-crown-6-ether (DB18C6)

Dibenzo-ether (DE)

Diffusivity (D)

Solubility (S)

Dibenzo-crown ether (DCE)

Bean Town Chemical (BTC)

Ethanol (EtOH)

N,N-Dimethylformamide (DMF)

n-Butanol (BuOH)

Tetrahydrofuran (THF)

Dichloromethane (DCM)

Dibenzo-24-crown-8-ether (DB24C8)

Dibenzo-30-crown-10-ether (DB30C10)

ACKNOWLEDGEMENTS

I greatly appreciate this opportunity to thank my peers, colleagues, and mentors, without whom this thesis could not have been made. Jason Bara greatly aided in the refinement of this research due his expertise in gas separation and insights into improvements of synthesis reactions. I would like to thank my thesis committee members, Prof. Steven Weinman and Prof. Paul Rupar for aiding me in completing my thesis reviewing my work. And many thanks to Dr. Sourav Chatterjee for his education in the synthesis and experimental techniques used for this research.

Also, I would like to thank my family for all their financial and emotional support throughout all my education. Without their support, the thesis would not have been possible.

CONTENTS

LIST OF TABLES

LIST OF FIGURES

LIST OF SCHEMES

1.0 INTRODUCTION

For decades, the rise in carbon dioxide (CO_2) emissions from intensive industrialization has become an increasing concern for global warming[1]. To counter this rising issue, several methods, such as solvent absorption[2], physical adsorption[3], and cryogenic distillation[4], have been implemented across many industries and power production to remove CO_2 from flue gas. However, these techniques have largely been unfavorable due to high maintenance cost and long-term investment. Membrane gas separation methods hold promise in reducing the cost of separation by low production price, passive gas transport, and ease of industrial scaling[5].

Many polymer membranes such as pentiptycene[6], phosphazene[7], and many others[8-10], have been under extensive study for their gas separation potential. Currently membranes with Tröger's base (TB)-linked polymer have been used for separation of H_2, He, and, CO_2[11-12]. The purpose behind these studies is the development of membranes with high permeability and selectivity towards the desired gas to be separated. Permeability is increased through an increased an increased separation between polymer segments or free volume[13] while selectivity is increased by the rigidity in the membrane[14].

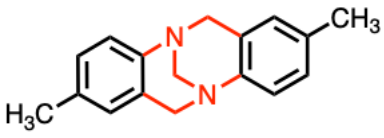

Figure 1: Example of Tröger's Base Linkage (linkage colored red)

Polymer membranes selectively separate gases from mixtures through two main mechanisms: diffusivity and solubility. Diffusivity (D) is ability of a molecule to move through the membrane which generally correlate with size of the molecule, while solubility (S) is the ability of a molecule to dissolve in the polymer membrane based on thermodynamic properties and intermolecular interactions.

TB polymers utilize both membrane rigidity and increased free volume in polymer to provide both high permeability and selectivity without compromising either. The TB linkages hold these properties due to the V-shaped hydrophobic cavities constructed by the perpendicular attachment of two benzene rings[15]. Several recent studies have utilized TB polymers for these useful properties[16-18]. However, the TB polymer membranes do not intrinsically have selectivity toward CO_2 separation and rely on the monomer for such properties.

The implementation of dibenzo-crown ethers as the base monomer contributes to the permeability of CO_2 due to the addition of double-strands of ethylene oxide chains in the molecule. The Lewis basic ether O atoms are known to interact with the Lewis acidic CO_2 molecules[19-20] By applying this CO_2-philic property into the polymer membranes CO_2 selectivity can be increased. From this analysis dibenzo-18-crown-6-ether (DB18C6) was selected due to its wide range study and large commercial production[21-22].

In this work TB-linked DB18C6 polymer membranes are prepared and utilized in gas separation. Also, a TB-linked dibenzo-ether (DE) polymer membrane is prepared and tested to compare the permeability and selectivity changes between the more rigid double-stranded DCE membrane and a looser single-stranded membrane.

2.0 BACKGROUND

2.1 Dibenzo-crown ethers

Dibenzo-crown ethers (DCEs) were first discovered in 1967 by Pederson in his research on the catalytic activity of vanadium and copper in multidentate ligands[23]. Since that time DCE compounds have been refined and applied into a multitude of different industries and research applications. They are utilized for alkali metal ion transport[24-29] due to their ability to selectively bind to these ions.

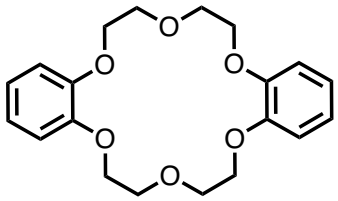

Figure 2: Dibenzo-18-crown-6-ether (DB18C6)

2.2 Tröger's Base

Tröger's Base (TB) (CAS: 529-81-7, IUPAC name: 2,8-Dimethyl-6H,12H-5,11-methanodibenzo [b,f] [1,5] diazocine) was discovered in 1887 from the reaction of p-toluidine and formaldehyde in acidic solution. TB synthesis has been a useful tool for host-guest chemistry research. TB compounds are chiral due to two nitrogen-containing stereogenic centers cultivating more and more interest from the field of supramolecular chemistry. The synthesis of TB derivatives is founded upon an acid induced reaction of an aromatic amine with formaldehyde (i.e.,

HCHO)[30] or equivalent forms (Scheme 1). The mechanisms of this synthesis are divided into aromatic moiety, which connects the benzene to the other reagent, and methano diazocine bridge, which forms the complete connection of the two amines. The TB linkage between the DCE creates a stable and chiral polymer from which the membrane can be formed creating rigidity in the membrane.

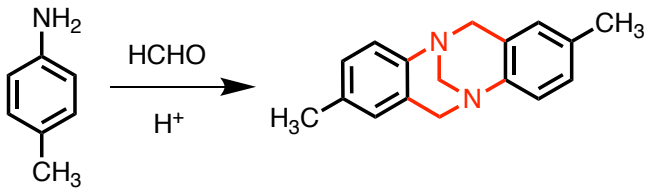

Scheme 1: Example Scheme of Tröger's Base Polymerization

2.3 Membrane Gas Separation

The mechanisms behind membrane gas separation are, at a basic level, a simple dynamic pressure system with a feed at high pressure and a feed at low pressure with the difference between the two pressures driving the system as seen in the article by Giorno[11]. The membrane generally acts like a sieve, allowing smaller molecules of the feed gas to enter more easily than larger molecules. When the feed gas is introduced into the system, it becomes either a retentate gas, which does not pass through, or permeate gas, which does pass through as shown in Figure 3. The effectiveness of a gas to pass through the membrane is called permeability. This permeability is composed of two parts; diffusion, which is determined by molecule and pore size, and solubility, which is determined by the intermolecular forces between the molecule and membrane. There are three main mechanisms that determine the diffusion of molecules across the membrane:

1) Knudsen Diffusion: at very low pressures smaller molecules pass through more quickly in membranes with large pores.

2) Molecular Sieving: the pores of the membrane are so small that only one component can pass through

3) Solution-Diffusion: the most common mechanism across all membranes, the feed gas is dissolved into the membrane then diffused through, both at different rates, this occurs as the pores in the membrane appear and disappear relative to the movement of the particles

The mechanism a membrane utilizes are revealed through experimentation however, the inclusion of the CO_2-philic ether groups in the membranes forced us to test for the solubility of the gas through the membrane.

This leads to the final goal of this gas separation: selectivity. The selectivity of a gas is the permeability of itself versus another gas determining the preference of the membrane[12]. The discovery of a membrane's selectivity of certain gases of others determines the possible uses that membrane may have. For instance, a membrane with a high selectivity towards hydrogen gas and no other gases would perform well if the separation of hydrogen from other gases was desired.

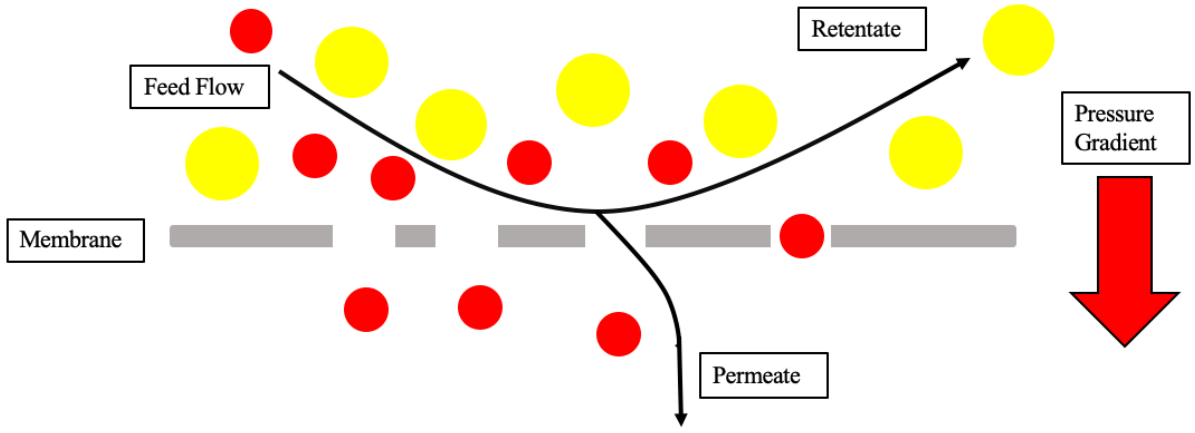

Figure 3: Membrane Gas Separation Example, where a feed gas contacts a porous membrane across a pressure gradient and either passes through to become a permeate gas or is unable to pass through and becomes a retentate gas

2.4 Crown Ether Polymers

The inspiration for studying this particular polymer came from an article written by Dr. Fraser Stoddart's group in 2018[21]. In this article, a TB-linked DB18C6 polymer was utilized for the ion transport of protons in a water medium for proton exchange fuel cells. The hydrophilic properties of DCE allow the polymer to transport protons from the anode facilitating higher battery efficiency. With these considerations, we presumed to apply the DCE properties of ion transport to the transport of the dipole gas CO_2 across a membrane.

3.0 METHODOLOGY

Table 1: Chemical Properties, Sources and Purities

Chemical Name, (Chemical Formula)	**CAS Number**	**Molecular Weight (g/mol)**	**Source/Purity displayed on container**
Catechol, ($C_6H_6O_2$)	120-80-9	110.1	Bean Town Chemical (BTC)/99%
Bis-2 (chloroethyl) ether, ($C_4H_8Cl_2O$)	111-44-4	143.0	BTC/99%
n-Butanol, (BuOH)	71-36-3	74.1	BTC/99.4%
Sodium Hydroxide, (NaOH)	1310-73-2	40.0	Fisher Scientific/ 98.1%
Hydrochloric Acid, (HCl)	7647-01-0	36.5	VWR Chemicals/36.5-38%
Chloroform, ($CHCl_3$)	67-66-3	119.4	Macron Chemical/99.8%
Acetic Acid, (AcOH)	64-19-7	60.1	Macron Chemical/glacial
Ethanol, (EtOH)	64-17-5	46.1	University Stock Room/100%
Hydrazine Hydrate, ($N_2H_4 \cdot H_2O$)	7803-57-8	32.0·18.0	BTC/98%
4-Nitrophenol, ($C_6H_5NO_3$)	100-02-7	139.1	BTC/99%
Triethylene glycol, ($C_6H_{14}O_4$)	112-27-6	150.2	BTC/99%
Potassium carbonate, (K_2CO_3)	584-08-7	138.2	BTC/99%

N,N-Dimethylformamide, (DMF)	**68-12-2**	**73.1**	**VWR Chemicals/99.8%**
Dimethoxymethane, $_{O2}$(DMM)	109-87-5	76.1	VWR Chemicals/99.8%
Triflouroacetic acid, $_{O2}$(TFA)	76-05-1	114.0	Alfa Aesar/99%
Ammonium Hydroxide, (NH_4OH)	1336-21-6	35.0	VWR Chemicals/28-30%
4-Toluenesulfonyl Chloride, (TsCl)	98-59-9	190.7	Alfa Aesar/98%
Potassium Hydroxide, (KOH)	1310-58-3	56.1	BTC/99%
Tetrahydrofuran, (THF)	109-99-9	72.1	Macron/99%
Dichloromethane, (DCM)	75-09-2	85.0	VWR Chemicals/99%

3.1 Synthesis of DB18C6

This procedure was obtained from Mane[32]. Catechol (29.7 g, 270 mmol) was added to a 1000 mL three-neck round bottom flask along with 180 mL of n-BuOH and agitated until the catechol dissolves. NaOH (10.95 g, 270 mmol) was added and the solution was heated at reflux (~117 ºC). During the increase in temperature, a solution of bis-2 (chloroethyl) ether (19.95 g, 140 mmol) and 18 mL of n-BuOH was prepared. Soon after the temperature reaches 117 ºC, the solution of bis-2 (chloroethyl) ether in n-BuOH was added dropwise over 2 h to the original solution, after which the solution was left under reflux for 1 hour with no other change. Then another 10.95 g (270 mmol) of NaOH was added to the solution, after the reaction temperature

was lowered to 90 ºC, it left for 1 h. Finally, a final solution of 19.95 g (140 mmol) of bis-2 (chloroethyl) ether and 18mL of n-BuOH was added dropwise over 2 h and then left for 16 h under reflux. Over the course of the wait the reaction as depicted in Figure 10 takes place. The synthesis was confirmed by ATR-FTIR spectrum (Appendix A Figure 1A).

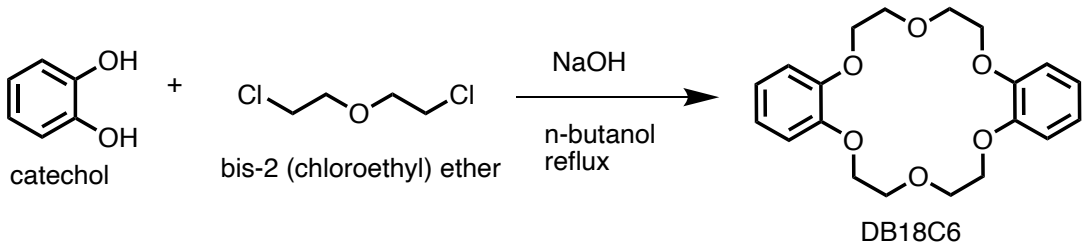

Scheme 2: Reaction Scheme for the synthesis of DB18C6

Proceeding the wait time, 1.34 mL of 12 M HCl was added to the solution for the acidification of the solution. 10 min afterward the solution was put under distillation for the removal of most of the n-butanol in the solution. Deionized water was added as a replacement for the product to undergo vacuum filtration and washed with alternating solvents of distilled water and acetone until a grey-white solid was obtained. This was the monomer DB18C6 with an average yield of 36.3%.

3.2 Nitration of DB18C6

For the nitration, 5.1 g (14.15 mmol) of DB18C6 was placed into a solution of 105 mL of chloroform and 75 mL of acetic acid in a 250 mL round-bottom flask[12]. The solution was stirred and dissolved, then a mixture of acetic anhydride and nitric acid was added dropwise. The reaction was set to reflux for 5 h at ~50 ºC. After, the reaction was filtered and recrystallized at 150 ºC in dimethylformamide (DMF). Finally, the solvent was removed under vacuum to obtain a white powder of di(nitrobenzo)-18-crown-6-ether (DNB18C6).

To verify the completion of the reaction, H^1-NMR (DMSO-d_6) and ATR-FTIR spectra were taken. In the H^1-NMR spectrum (Appendix B, Figure B.1), peaks at 7.24 ppm, 7.72 ppm, and 7.89 ppm indicate the presence of aromatic H, while the peaks at 3.88 ppm and 4.21 ppm point to the alkyl H.

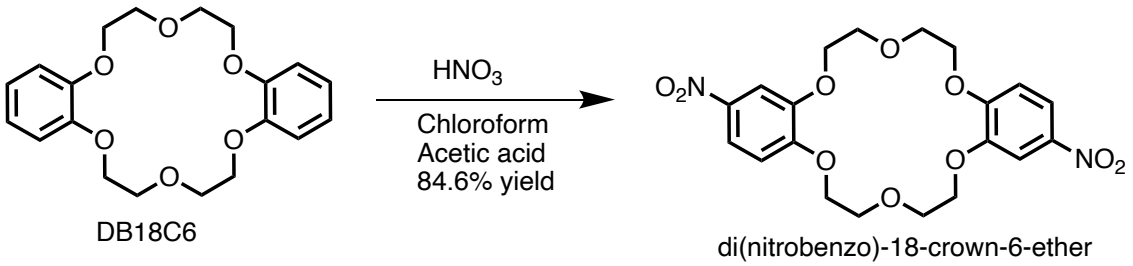

Scheme 3: Nitration of DB18C6

3.3 Reduction of Dinitrobenzo-18-crown-6-ether

Approximately 5 g (11.96 mmol) of the above-produced DNB18C6 was dissolved in 170 mL of EtOH along with 0.5 g of 10% Pd/C. The mixture was stirred with a magnetic stir bar and refluxed at 90 ºC as 35 mL (700 mmol) of hydrazine hydrate was added over 20 min[13]. The mixture was then left under reflux for 5 h. The Pd/C was removed by filtration and washed with EtOH to produce a white crystalline product after crystallization at 80°C under vacuum. Furthermore, the diaminobenzo-18-crown-6-ether was verified with H^1-NMR spectrum (Appendix B Figure B.2) and ATR-FTIR spectrum (Appendix A Figure A.1). For the H^1-NMR spectrum, the appearance of the peak at 4.63 ppm confirms the formation of the amine group as all other relevant peaks remain the same.

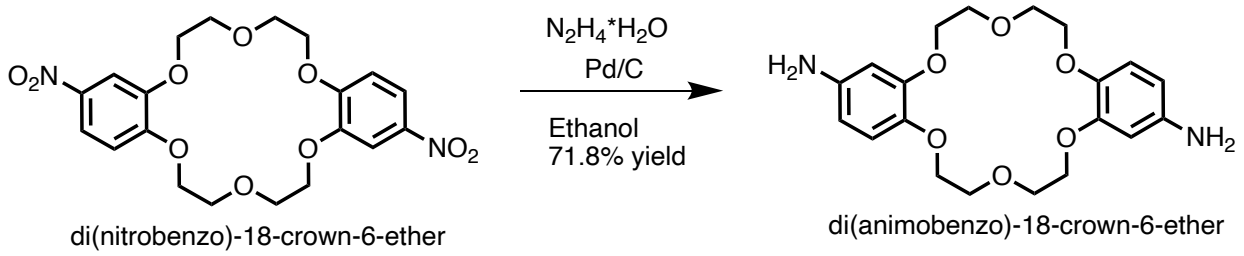

Scheme 4: Reaction Scheme of the Reduction of Dinitrobenzo-18-crown-6-ether

3.4 Synthesis of Triethylene glycol di(p-toluenesulfonate)

A solution of triethylene glycol (15.4 g, 102.8 mmol), TsCl (58.8 g, 308.8 mmol), and THF (200 mL) was formed in a 1000 mL round-bottom flask with stirring from magnetic stir bar. After cooling the solution to 0 °C, a solution of KOH (38.0 g, 678.4 mmol) and H_2O (60 mL) was added dropwise over 30 min. Then, the solution temperature was raised to room temperature and stirred for 2 d. The resultant liquid was partitioned between H_2O (200 mL) and DCM (250 mL) with the organic layer being washed with H_2O (400 mL), brine (400 mL) and dried with $MgSO_4$. The filtered dried solution was mixed with methanol to crystalize the product, which after filtration was a white crystal and a yield of 45.9%. This reaction was shown in Scheme 5. Characterization was not taken for this reaction.

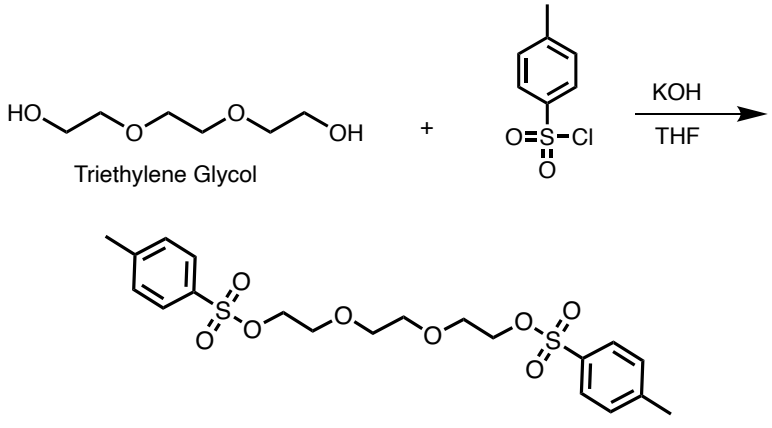

Scheme 5: Reaction Scheme of Triethylene glycol di(p-toluenesulfonate)

3.5 Synthesis of Dinitrobenzene Ether

This procedure was acquired from Xi[33]. First, 4.17 g (30.0 mmol) of 4-nitrophenol and 12.42 g (89.87 mmol) of K_2CO_3 added to 100 mL of DMF in a 500 mL round-bottom flask and stirred with a magnetic bar at 40 °C for 10 min to dissolve the components. After dissolution, the reaction was set to reflux at 90 °C while 21.25 g (46.35 mmol) of triethylene glycol di(p-toluenesulfonate) was added dropwise. The mixture was left to reflux for 18 h then was filtered and washed to produce a pale-yellow powder with a yield of 43.0%. Characterization was performed with FTIR spectrum (Appendix A Figure A.2) and H^1-NMR spectrum (Appendix B Figure B.3).

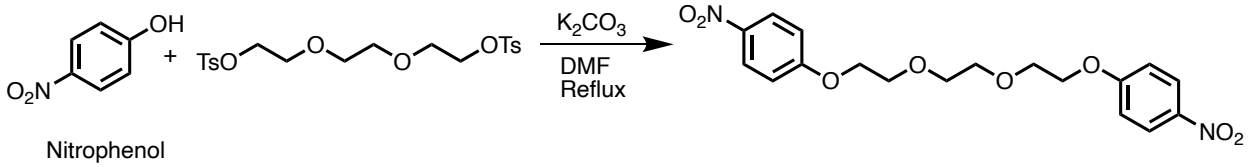

Scheme 6: Reaction Scheme of Dinitrobenzo-ether

3.6 Reduction of Dinitrobenzene Ether

To perform the reduction, 5 g (12.74 mmol) of dinitrobenzene ether were dissolved in 170 mL of ethanol (EtOH) together with 0.5 g of 10% Pd/C. The solution was stirred and refluxed at 90 °C while 35 mL (700 mmol) of hydrazine hydrate was added dropwise over 20 min and left to reflux for 5 h. The Pd/C was removed by filtration and washed with EtOH to produce a white

crystalline product after crystallization at 80 °C under vacuum. FTIR (Appendix A Figure 2A) and H^1-NMR spectra (Appendix B Figure 2B) were taken to confirm product formation.

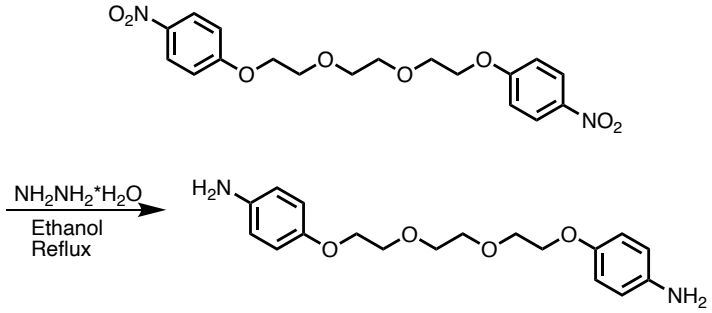

Scheme 7: Reaction Scheme of the Reduction of Dinitrobenzo-ether

3.7 Synthesis of Polymer

Each monomer is mixed together with . in a round-bottom flask in an ice bath. TFA is then added dropwise over 15 min at 0 °C and vigorously stirred with a magnetic stir bar after which the reaction temperature is left to rise to room temperature and stirred for 48 h. The resulting liquid was added to an aq. NH_4OH solution and stirred for 1 h, then filtered, soaked in water, washed with MeOH, THF, and acetone, before being dried at 80 °C under vacuum for collection. The schemes of DB18C6 and 1,2-Bis[2-(4-aminophenoxy) ethoxy] ethane for this reaction are shown in Schemes 8 and 9 respectively. Both polymers were characterized by ATR-FTIR spectrum. The formation of Tröger's base linkage is supported by the appearance of C-N stretching bands at points 1360 and 1090 cm^{-1}. (Appendix A Figures A.1 and A.2).

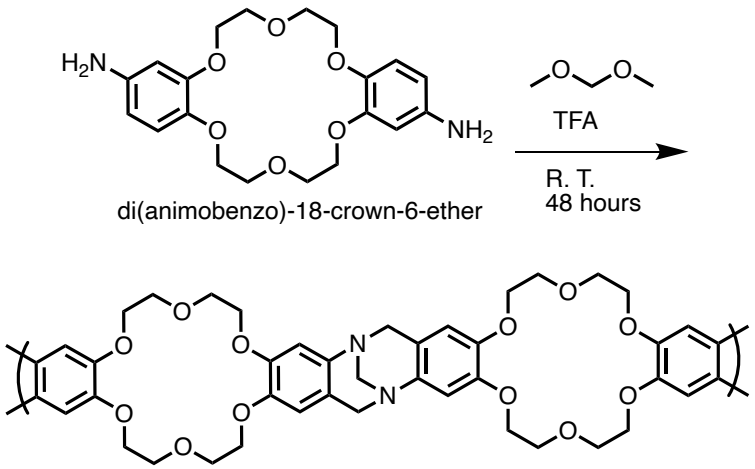

Scheme 8: Reaction Scheme of Tröger's Base Polymerization of Binitrobenzo-18-crown-6-ether

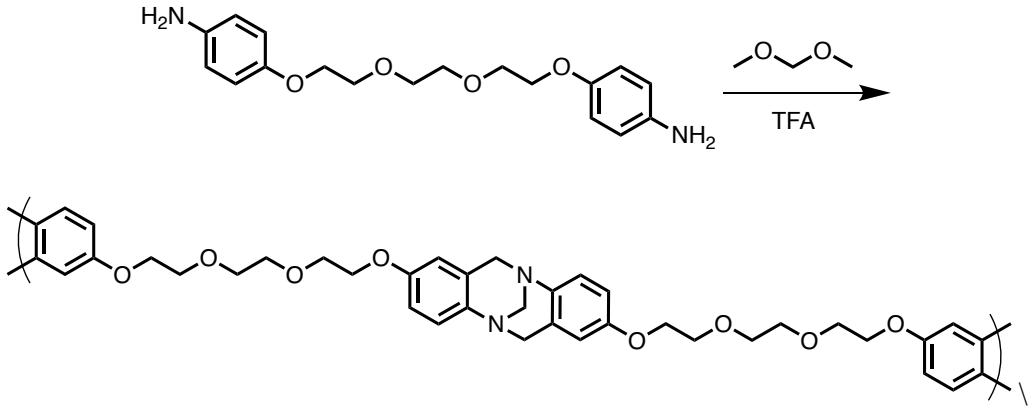

Scheme 9: Reaction Scheme of Tröger's Base Polymerization of Biaminobenzo-ether

3.8 Membrane Casting

Each membrane was cast by dissolving the synthesized polymer in $CHCl_3$ and poured into a 60-mm diameter petri dish. The solvent was permitted to evaporate completely over night to give membranes of 0.09 mm thickness.

3.9 Membrane Gas Separation

To test the permeability of gases through the membrane, all separation experiments were performed using an in-house-made high pressure cell based on established literature methods (Figure 4).

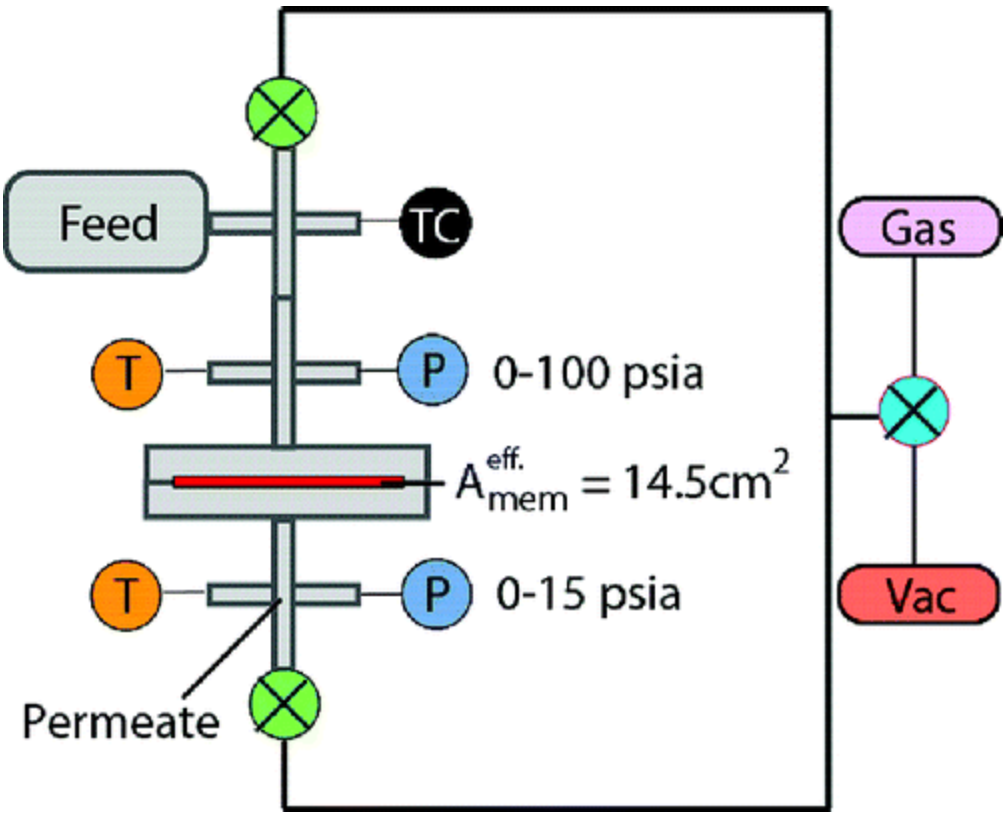

Figure 4: Diagram of Gas Separation Equipment[34]

The membranes were masked with aluminum foil tape to control the area of the membranes exposed to the feed gas and protect them from breaking through direct contact with the o-ring, though breaks still can occur. All experiments were performed at room temperature (~295 K) in this work. The membranes in the masks were placed into the membrane holder and the system was

then sealed with bolts around the holder. The vacuum pump was activated to purge the system of residual air and the outflow valve was closed. Next, the chambers were filled with the experiment gas until a predetermined pressure was reached as relayed by pressure sensors attached to the chamber. Once the pressure threshold was reached, the feed valve was closed to close off the membrane chamber from the rest of the system. As soon as the feed valve was closed the data collection of pressure of gas that passed through the membrane was taken over time. Once the chamber reached equilibrium or the sufficient data was collected for an accurate measurement, both valves were opened and the gas was vacuumed out to be replaced by the next testing gas. This process was repeated for every tested gas. This data was then formed into a cumulated volume over time graph. The data of the graph applied to the equation for permeability.

The permeability of a gas is measured by the rate of gas cumulative that has passed through the membrane as shown below by Eqn. 1:

$$P = \frac{V_{perm}\Delta P}{AtRT\phi}\frac{I}{\Delta p_i} \qquad \text{----------(1)}$$

where V_{perm} is the volume of permeate (cm^3), ΔP is the rise in permeate pressure (Pa), A is the effective membrane area (cm^2), t is time (s), T is the temperature (K), R is the gas constant ($cm^3 \cdot Pa \cdot K^{-1} \cdot mol^{-1}$), ϕ is the support porosity (g/cm^2), I is the membrane thickness (cm), Δp_i is the driving force exerted by the pressure gradient on the membrane($m^3 \cdot Pa \cdot g^{-1}$), and P is the permeability in barrer ($mol \cdot m \cdot m^{-2} \cdot s \cdot Pa$).

The diffusivity was calculated separately through the Eqn. 2:

$$D = \frac{I^2}{6\theta} \qquad \text{----------(2)}$$

where l is the membrane thickness (cm), θ is the time lag (s), and D is the diffusivity (cm^2/s).

The solubility was calculated through the Eqn. 3:

$$P = D * S \qquad \text{----------(3)}$$

where D is diffusivity (10^{-8} cm^2/s), S is solubility (cm^3 (STP) cm^{-3} cm^{-1} Pa^{-1}), and P is permeability (barrer, mol cm cm^{-2} s Pa).

Finally, the selectivity was calculated as a simple ratio as shown with the equation 4:

$$\alpha_{ij} = \frac{P_i}{P_j} \qquad \text{----------(4)}$$

where P_i is the first gas permeability, P_j is the second gas permeability, and $\alpha_{i/j}$ is the selective permeability of gas i over gas j.

4.0 RESULTS AND DISCUSSION

4.1 Membrane Analyzation

The DB18C6 membrane was hard to handle and manipulate making testing difficult as the membrane was liable to break if care was not taken. This rigid nature was highly likely to be caused by the duel strands of ether connecting the two benzene rings together and Tröger's base-linkage. The combination of these two connections led to high rigidity due to the lack of rotation in the molecule.

The dibenzo ether membrane was far more flexible, being able to be bent before breaking. This property was caused by the single-strand ether connection which, unlike the double-stranded DB18C6, allows for the polymer backbone to rotate, increasing its flexibility. These properties hold importance in the application of these membranes, as a membrane that breaks will compromise the CO_2 separation. The solution to this may be to augment the DB18C6 membrane with ionic liquids to give more flexibility. Both membranes reported thicknesses of between 0.050 and 0.150 mm.

4.2 Tröger's Base DB18C6 Membrane Gas Separation

The data for the gas permeability of the membrane came from four feed gases, along with CO_2 which are hydrogen (H_2), oxygen (O_2), nitrogen (N_2), and methane (CH_4). These gases

were fed to membrane chamber to permeate through the membrane. The amount of the permeate volume accumulation over time were recorded and used to construct a graph like the one seen Figure 5. The data was then input into the equations for permeability, diffusivity, and solubility to produce Table 2.

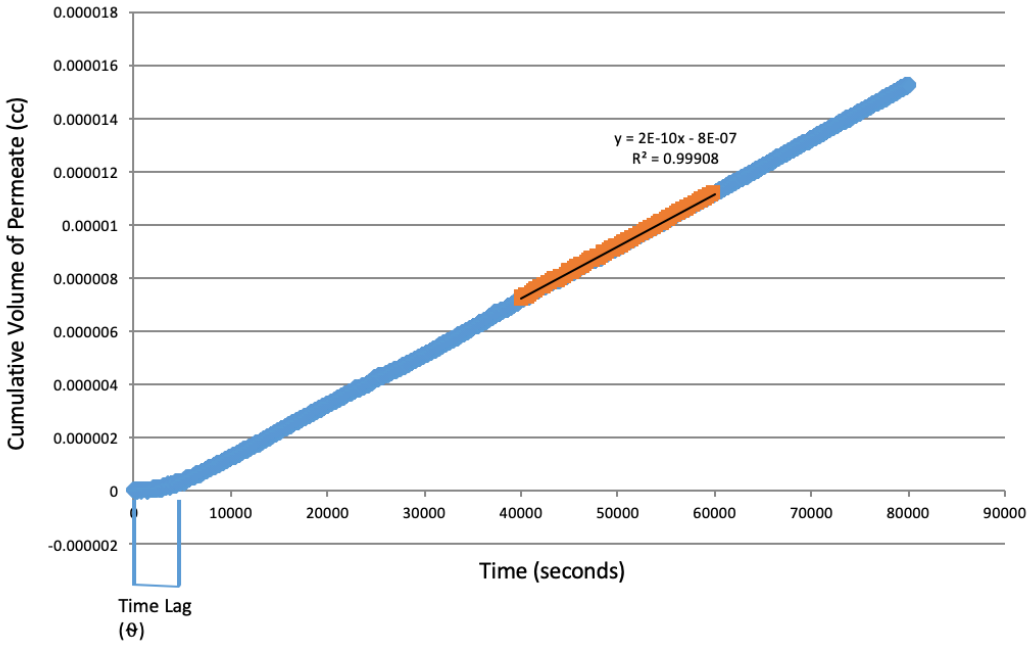

Figure 5: Typical Graph from Gas Separation Equipment[34]

Table 2: Tröger's Base-linked DB18C6 Permeability Data

Gas (Kinetic Diameter, Å)	**Diffusivity (10^{-8} cm^2/s)**	**Solubility ((STP) cm^{-1} Hg^{-1})**	**Permeability (barrer, mol·m ·m^{-2}·s·Pa)**
H_2 (2.34)	129	0.04	**5.38**
CO_2 (3.30)	0.60	3.40	**2.66**
O_2 (3.46)	2.07	0.23	**0.61**
N_2 (3.64)	0.50	0.35	**0.23**
CH_4 (3.80)	0.55	0.53	**0.19**

From the data collected, two immediate conclusions become apparent; the relationship between permeability and molecule size, and the comparison of the H_2 diffusivity and CO_2 solubility. This property has been show amongst other TB polymer membranes[15-16]. The gases that are used for separation each have different molecule diameters from the smallest H_2 (2.34Å) to the largest CH_4 (3.80Å) and these sizes correlate the permeability of each of the gases. This relationship follows the trend of: $P(CH_4) < P(N_2) < P(O_2) < P(CO_2) < P(H_2)$, and diameters: CH_4(3.80 Å) > N_2 (3.64 Å) > O_2 (3.46 Å) > CO_2 (3.3Å) > H_2 (2.34 Å), demonstrating an inverse relation between the diameter and permeability. This follows with gas separation principles as seen in Giorno[15]. The second observation depicts the diffusivity-controlled permeability of H_2 and solubility-controlled permeability of CO_2. This coincides with Quan[5], proving that the ether groups in DB18C6 did contribute to the facilitation of CO_2 transport across the membrane due the highly increased solubility of the CO_2 compared to the other gases.

Finally, the selectivity of each gas was obtained using the equation $\alpha_{1/2} = P_1/P_2$ providing the data for Figure 6. The CO_2 selectivity shows that CO_2 has a significantly higher rate of permeation than all other gases except H_2 demonstrating that the TB-DB18C6-membrane is applicable to preferred CO_2 separation. However, in comparison to other studies performed for the selective membrane gas separation of CO_2, the TB-DB18C6-Polymer membrane had a lower selectivity to CO_2/N_2 with 12.3 compared to the significantly higher 60 at a temperature of 30 °C as seen in the Poly (ethylene glycol) diglycidyl ether membrane of Quan[17].

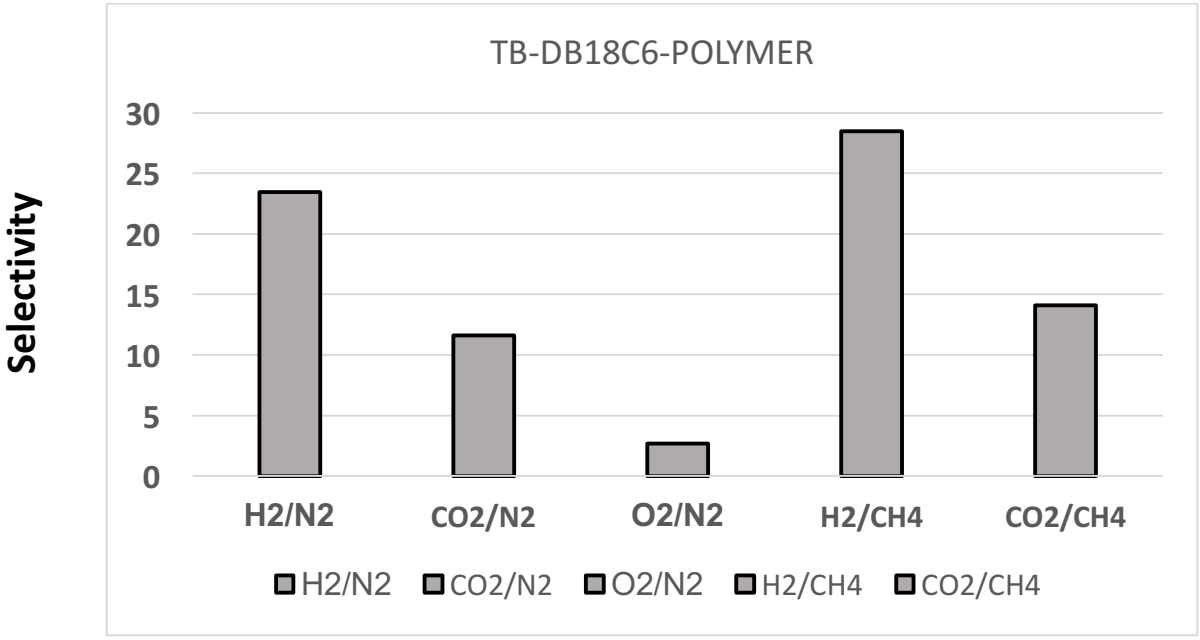

Figure 6: Bar Graph of TB-DB18C6-Polymer Gas Selectivity

4.3 Future Research

At the time of writing, the gas separation data for the single-strand dibenzo ether membrane has not been obtained. However, the same criteria will be applied, and the same five gases will be used for the feed streams. The membrane is predicted to have similar gas selectivity to the double-strand DCE membrane, but it will likely be more permeable to all the feed gases due to the capacity to rotate by the ether groups.

The exchange of the ether groups for alkyl groups has already begun to be explored with the planned synthesis of dibenzo crown alkane and dibenzo alkane. This change was proposed to determine to the effectiveness of the CO_2 ether groups to the theoretically weaker interaction of the alkane groups in CO_2 gas separation. These new monomers (as shown in Scheme 10) will be polymerized with Tröger's base linkages. In the long term, alterations to the structure based changes to hydroxide positions from ortho-position (catechol) to meta-position (resorcinol) or para-position (hydroquinone) as seen in Figure 7. As well as extensions to the ether groups

forming monomers such as dibenzo-24-crown-8-ether and dibenzo-30-crown-10-ether (Figure 8). These new configurations permit further testing on a possible relationship between crown size in the particle and permeability.

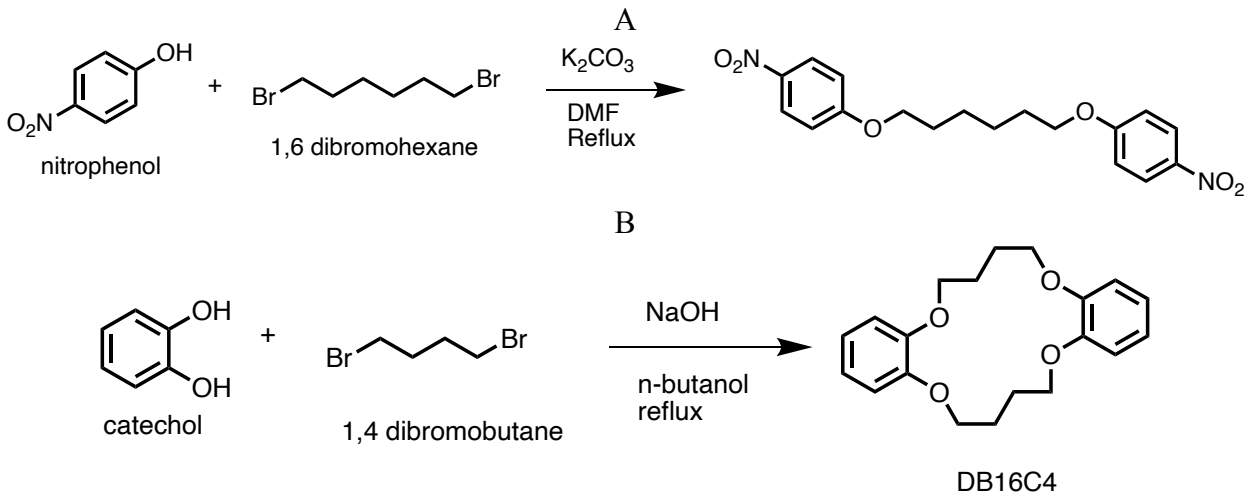

Scheme 10: Reaction Scheme of Dibenzo-alkane (A) and Bibenzo-16-crown-4-alkane (DB16C4) (B)

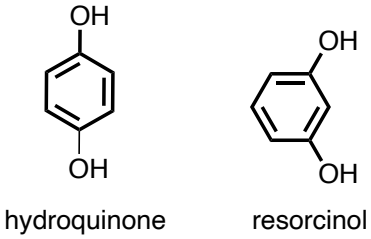

Figure 7: Molecular Structure of Hydroquinone and Resorcinol

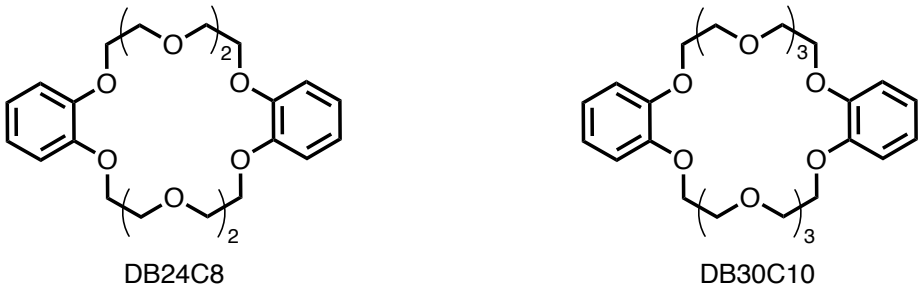

Figure 8: Molecular Structure of benzo-24-crown-8-ether (DB24C8) and dibenzo-30-crown-10-ether (DB30C10)

REFERENCES

1. Stocker, T.F., D. Qin, G.-K. Plattner, M. Tignor, S.K. Allen, J. Boschung, A. Nauels, Y. Xia, V. Bex, P.M. Midgley (eds.). *Climate Change 2013: The Physical Science Basis. Contribution of Working Group I to the Fifth Assessment Report of the Intergovernmental Panel on Climate Change* Cambridge University Press, Cambridge, United Kingdom and New York, NY, USA, 2013, p 1535

2. Hannah Ritchie, Max Roser, *CO_2 and Greenhouse Gas Emissions*. OurWorldInData.org. https://ourworldindata.org/co2-and-other-greenhouse-gas-emissions

3. Robert Czarnota , Ewa Knapik, Pawel Wojnarowski, Damian Janiga, Jerzy Stopa, *Carbon Dioxide Separation Technologies,* Arch. Min. Sci. 64, 2019, 3, p 487-498

4. Mohammad Songolzadeh, Mansooreh Soleimani, Maryam Takht Ravanchi, Reza Songolzadeh, *Carbon Dioxide Separation from Flue Gases: A Technological Review Emphasizing Reduction in Greenhouse Gas Emissions*, The Scientific World Journal vol. 2014, p 34

5. Rodney J. Allam, Rune Bredesentm, Enrico Drioli. *Carbon Dioxide Separation Technologies*, Carbon Dioxide Recovery and Utilization, 2003, p 53-120.

6. Hongjun Yang, Shuanshi Fan, Xuemei Lang, Yanhong Wang, Jianghua Nie, *Economic Comparison of Three Gas Separation Technologies for CO2 Capture from Power Plant Flue Gas*, Chinese Journal of Chemical Engineering, Volume 19, Issue 4, 2011, p 615-620

7. Tanner J. Corrado, et. al., *Pentiptycene-based ladder polymers with configurational free volume for enhanced gas separation performance and physical aging resistance*, PNAS, 2021 vol. 118 p 37

8. Shuangjiang Luo, Kevin A. Stevens, Jae Sung Park, Joshua D. Moon, Qiang Liu, Benny D. Freeman, Ruilan Guo. *Highly CO2-Selective Gas Separation Membranes Based on Segmented Copolymers of Poly(Ethylene oxide) Reinforced with Pentiptycene-Containing Polyimide Hard Segments,* ACS Applied Materials & Interfaces 2016 *8* (3), p 2306-2317

9. Anja. Car, Chrtomir. Stropnik, Wilfredo Yave, Klaus-V. Peinemann. *PEG modified poly(amide-b-ethylene oxide) membranes for CO2 separation*, Journal of Membrane Science, Volume 307, Issue 1, 2008, p 88-95

10. Mari Vinoba, Margandan Bhagiyalakshmi, Yousef Alqaheem, Abdulaziz A. Alomair, Andrés Pérez, Mohan S. Rana. *Recent progress of fillers in mixed matrix membranes for CO2 separation: A review,* Separation and Purification Technology, Volume 188, 2017, p 431-450

11. Michele Galizia, Won Seok Chi, Zachary P. Smith, Timothy C. Merkel, Richard W. Baker, Benny D. Freeman, *50th Anniversary Perspective: Polymers and Mixed Matrix Membranes for Gas and Vapor Separation: A Review and Prospective Opportunities*, Macromolecules 2017 *50* (20), p 7809-7843

12. Xiaofan Hu, Won Hee Lee, Jiayi Zhao, Joon Yong Bae, Ju Sung Kim, Zhen Wang, Jingling Yan, Yongbing Zhuang, Young Moo Lee, *Tröger's Base (TB)-containing polyimide membranes derived from bio-based dianhydrides for gas separations*, Journal of Membrane Science, Volume 610, 2020, 118255

13. Wang, Zhenggong et al. *Tröger's Base-Based Microporous Polyimide Membranes for High-Performance Gas Separation*. ACS Macro Letters 3 (2014): p 597-601.

14. Giorno L., Drioli E., Strathmann H. *The Principle of Gas Separation*. Encyclopedia of Membranes. 2015
Marc B. Lande, Joanne M. Donovan, Mark L. Zeidel, *The Relationship between Membrane Fluidity and Permeabilities to Water, Solutes, Ammonia, and Protons*, J. GEN. PHYSIOL, Volume 106, 1995, p 67-84

15. Benny D. Freeman, *Basis of Permeability/Selectivity Tradeoff Relations in Polymeric Gas Separation Membranes*, Macromolecules, volume *32* (2) 1999, p 375-380

16. Ögmundur Vidar Rúnarsson, Josep Artacho, Kenneth Wärnmark, *The 125th Anniversary of the Tröger's Base Molecule: Synthesis and Applications of Tröger's Base Analogues*, Volume 2012, Issue 36, 2012, p 7015-7041

17. Zhiyang Zhu, Junjie Zhu, Jianxin Li, and Xiaohua Ma, *Enhanced Gas Separation Properties of Tröger's Base Polymer Membranes Derived from Pure Triptycene Diamine Regioisomers*, Macromolecules 2020 53 (5), p 1573-1584

18. Lee M. Bezzu, CG Carta, M Bernardo, P Clarizia, G Jansen, JC McKeown, *Enhancing the Gas Permeability of Tröger's Base Derived Polyimides of Intrinsic Microporosity,* Macromolecules, vol. 49, no. 11, 2016, p 4147-4154

19. Deng, Jing et al. *H2-selective Troger's base polymer based mixed matrix membranes enhanced by 2D MOFs*. Journal of Membrane Science 2020 Vol. 610, 118262.

20. Shuai Quan, Songwei Li, Zhenxing Wang, Xingru Yan, Zhanhu Guo, Lu Shao, *A bio-inspired CO2-philic network membrane for enhanced sustainable gas separation*, J. Mater. Chem. A, 2015, Issue 3, 13758

21. Peter W. J. Morrison, et al. *Crown Ethers: Novel Permeability Enhancers for Ocular Drug Delivery?,* Molecular Pharmaceutics 2017 Vol. 14 Issue 10, p 3528-3538

22. Fornaciari Iljadica, María C, et al. *Investigation on the chemical behaviour of a crown ether irradiated in high gamma radiation fields.* Radiochimica Acta 2005 vol. 93 p 601 - 603.

23. Charles J. Pedersen, *The Discovery of Crown Ethers*, *SCIENCE,* 1988, Vol. 241, Issue 4865, p 536-540

24. Pooja Sahu, Sk. M. Ali, Jayant K. Singh*, Structural and dynamical properties of Li+ - dibenzo-18-crown-6(DB18C6) complex in pure solvents and at the aqueous-organic interface,* J Mol Model 2014 20:2413

25. Hasmukh A. Patel, John Selberg, Dhafer Salah, Haoyuan Chen, Yijun Liao, Siva Krishna Mohan Nalluri, Omar K. Farha, Randall Q. Snurr, Marco Rolandi, J. Fraser Stoddart, *Proton Conduction in Tröger's Base-Linked Poly(crown ether)s,* ACS Applied Materials & Interfaces 2018 Vol. 10 Issue 30, p 25303-25310

26. Wang, Da-Ming et al. *Synthesis and Characterization of Alkali Metal Ion-Binding Copolymers Bearing Dibenzo-24-crown-8 Ether Moieties.* Polymers vol. 10,10, 2018 p 1095.

27. Yi Ying, Wang Yuting, Liu Hui. *Preparation of new crosslinked chitosan with crown ether and their adsorption for silver ion for antibacterial activities*. Carbohydrate Polymers 2003 Issue 53. p 425-430.

28. Cantrill SJ, Fulton DA, Heiss AM, Pease AR, Stoddart JF, White AJ, Williams DJ. *The influence of macrocyclic polyether constitution upon ammonium ion/crown ether recognition processes*. Chemistry. 2000 Vol. 6 Issue 12, p 2274-87

29. Hanlie R. Wessels, Harry W. Gibson, *Multi-gram syntheses of four crown ethers using K+ as templating agent,* Tetrahedron, Vol. 72, Issue 3, 2016, p 396-399

30. Bohumil Dolenský, José Elguero, Vladimír Král, Carmen Pardo, Martin Valík, *Current Tröger's Base Chemistry*, Advances in Heterocyclic Chemistry, Academic Press, Volume 93, 2007, p 1-56

31. Irving Sucholeiki, Vincent Lynch, Ly Phan, Craig S. Wilcox, *Chemistry of synthetic receptors and functional group arrays. 7. Molecular armatures. Synthesis and structure of Troeger's base analogs derived from 4-, 2,4-, 3,4-, and 2,4,5-substituted aniline derivatives*, The Journal of Organic Chemistry 1988, Vol. 53 Issue 1, p 98-104

32. Sachin Mane, Surendra Ponrathnam, Nayaku Chavan. *Selective Solid-Phase Extraction of Metal for Water Decontamination.* J. Appl. Polym. Sci. 2016, Vol. 132, 42849

33. Xi Shu, Ruyu Wang, Yu Fan, Shoujian Li. *Chao Huang,Macrocyclic bis-urea receptor: Synthesis, crystal structure and phosphate binding properties*,Tetrahedron Letters, Vol. 60, Issue 10, 2019, p 729-733

34. Jason E. Bara, Sonja Lessmann, Christopher J. Gabriel, Evan S. Hatakeyama, Richard D. Noble, Douglas L. Gin. *Synthesis and Performance of Polymerizable Room-Temperature Ionic Liquids as Gas Separation Membranes*, Industrial & Engineering Chemistry Research 2007 Vol. 46 Issue 16, p 5397-5404

APPENDICES

Appendix A: FTIR Spectra

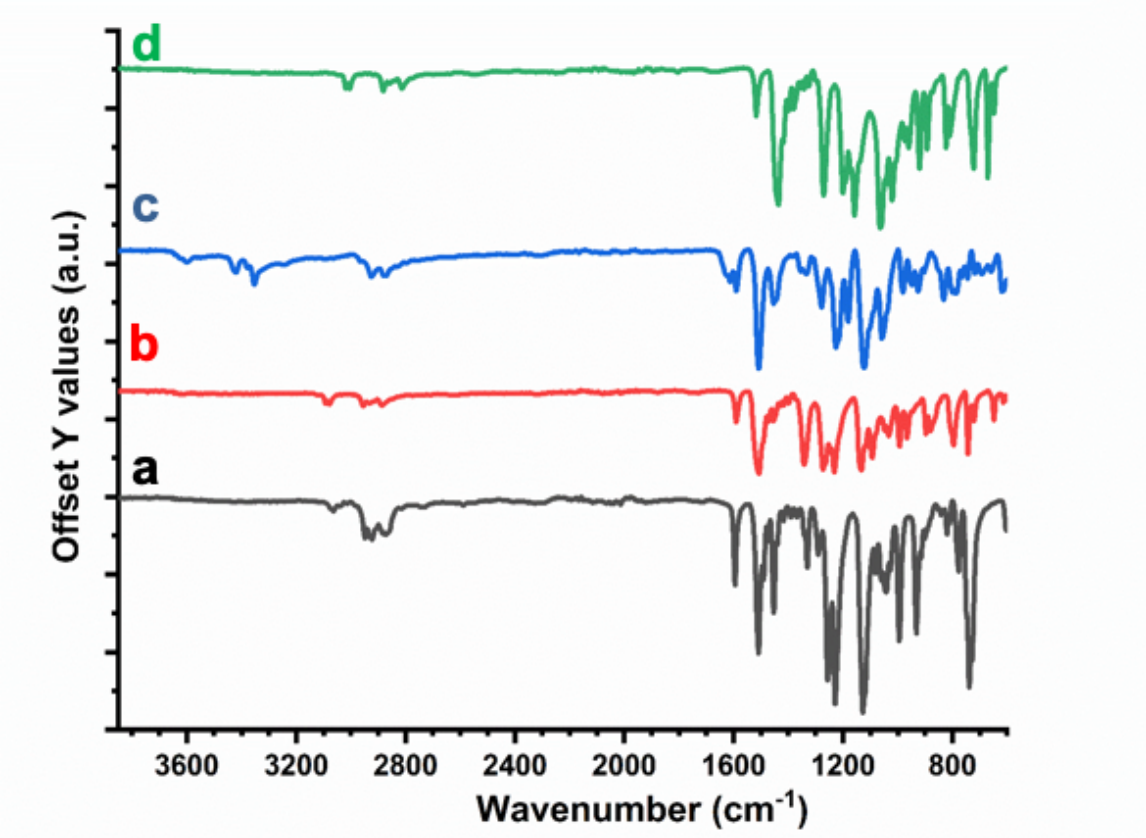

Figure A. 1: FTIR spectra of DB18C6 products. (a) DB18C6, (b) dinitroDB18C6, (c) diaminoDB18C6, (d) TB-linked DB18C6 polymer

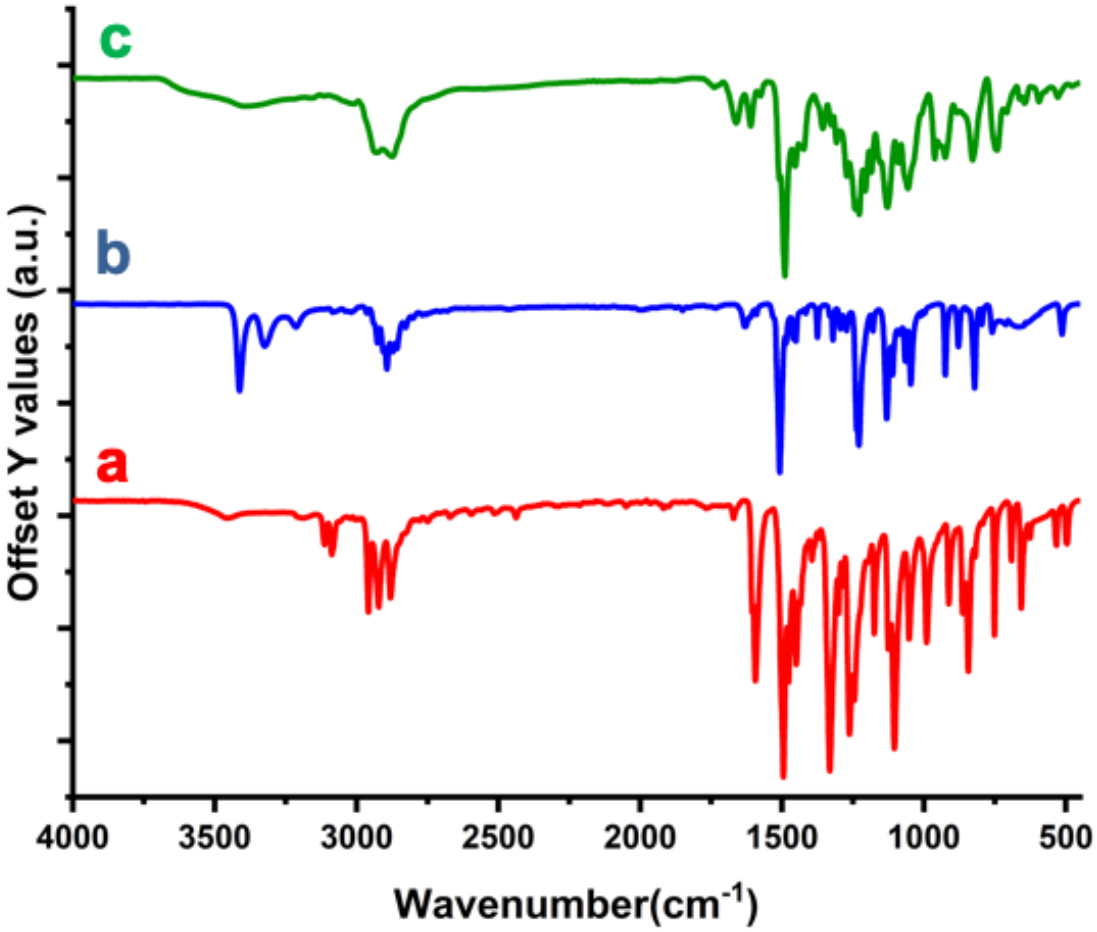

Figure A. 2: FTIR spectra of single-strand Dibenzo-ether products. (a) dinitroDibenzo-ether, (b) diaminoDibenzo-ether, (c) TB-linked Dibenzo-ether polymer

Appendix B: H^1-NMR Spectra

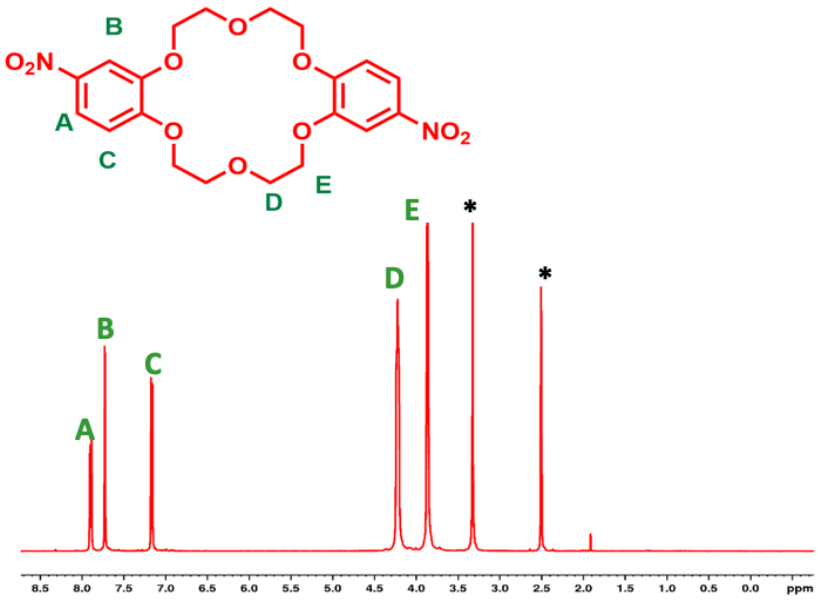

Figure B. 1: H^1-NMR Spectrum of Dinitrobenzo-18-crown-6-ether: Peaks A, B, C correlate to the aromatic hydrogens, Peaks D, E correlate to alkyl hydrogens, Asterisk (*) peaks relate to water and $DMSO_4$

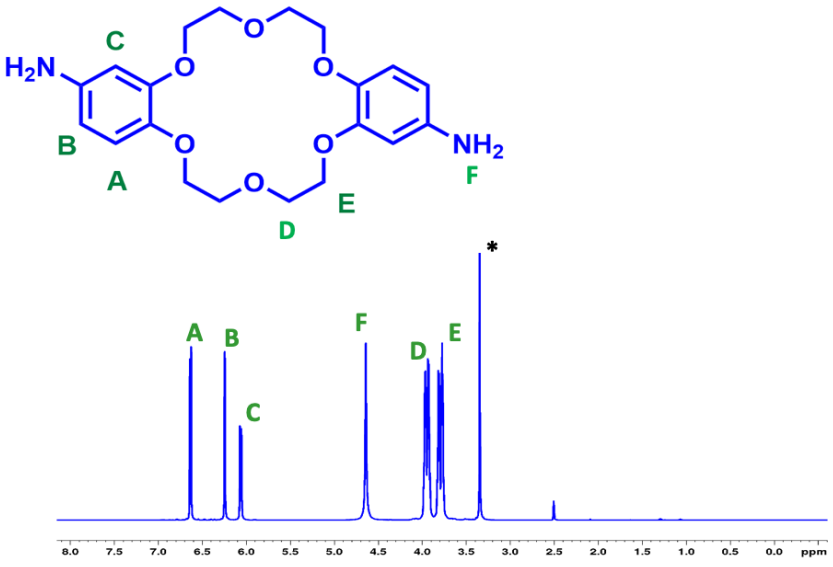

Figure B. 2: H^1-NMR Spectrum of Diaminobenzo-18-crown-6-ether: Peaks A, B, C correlate to the aromatic hydrogens, Peaks D, E correlate to alkyl hydrogens, Peak F correlates to the amine group hydrogen, Asterisk (*) peaks relate to water and $DMSO_4$

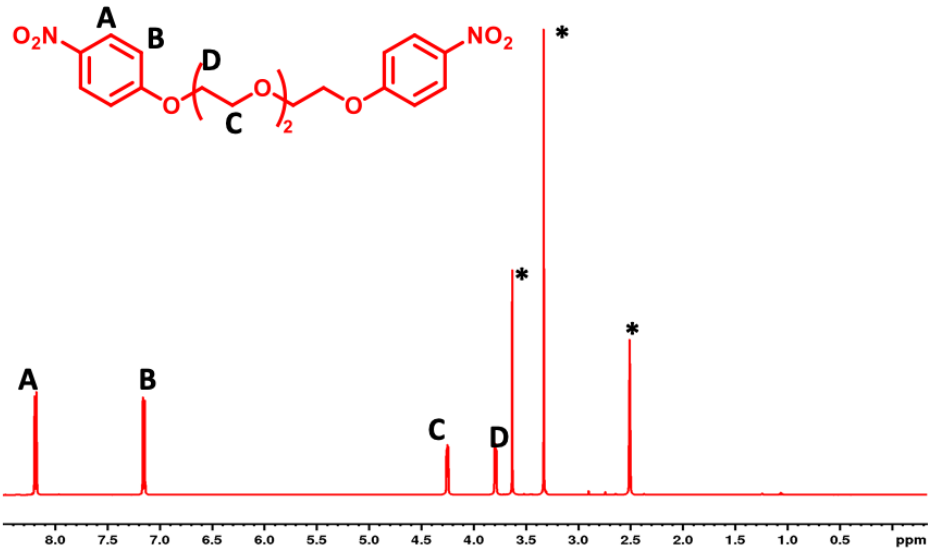

Figure B. 3: H[1]-NMR Spectrum of Dinitrobenzo-ether: Peaks A, B correlate to the aromatic hydrogens, Peaks C, D correlate to alkyl hydrogens, Asterisk (*) peaks relate to water and $DMSO_4$

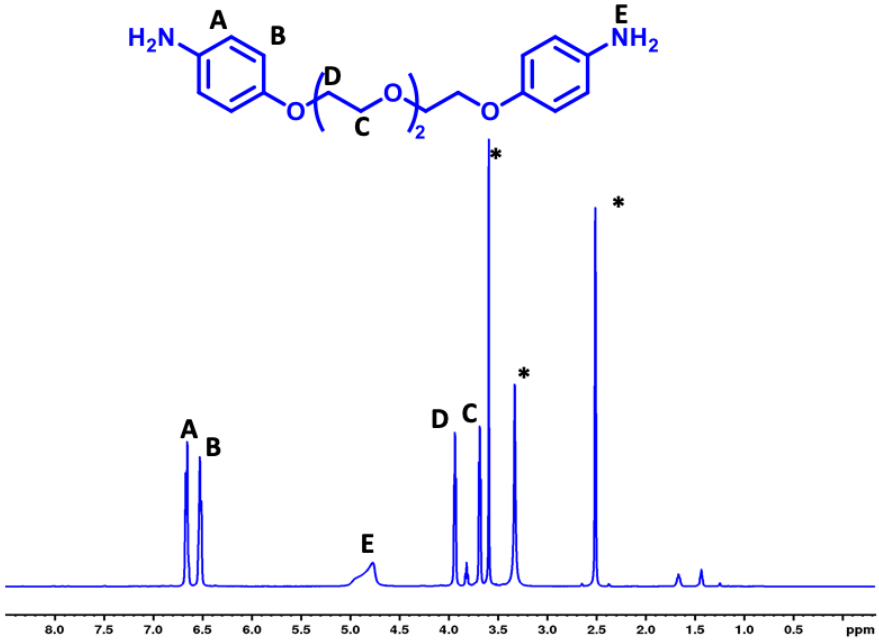

Figure B. 4: H[1]-NMR Spectrum of Diaminobenzo-ether: Peaks A, B correlate to the aromatic hydrogens, Peaks C, D correlate to alkyl hydrogens, Peak E correlates to the amine group hydrogen, Asterisk (*) peaks relate to water and $DMSO_4$